

## Supporting Information

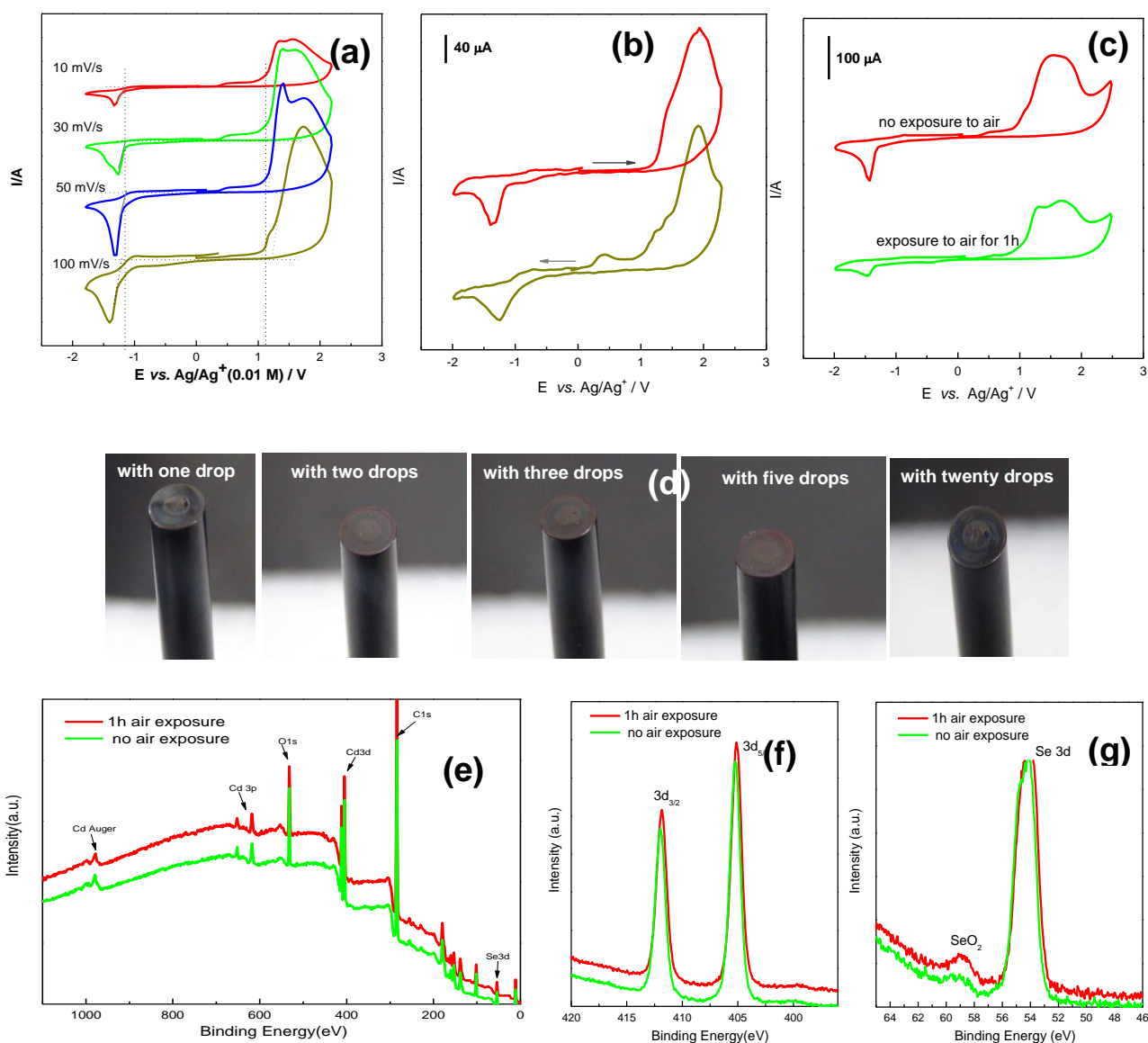
for

# Electrochemical Studies of the Size, Ligand and Composition Effect on the Band Structures of CdSe, CdTe and their Alloyed Nanocrystals

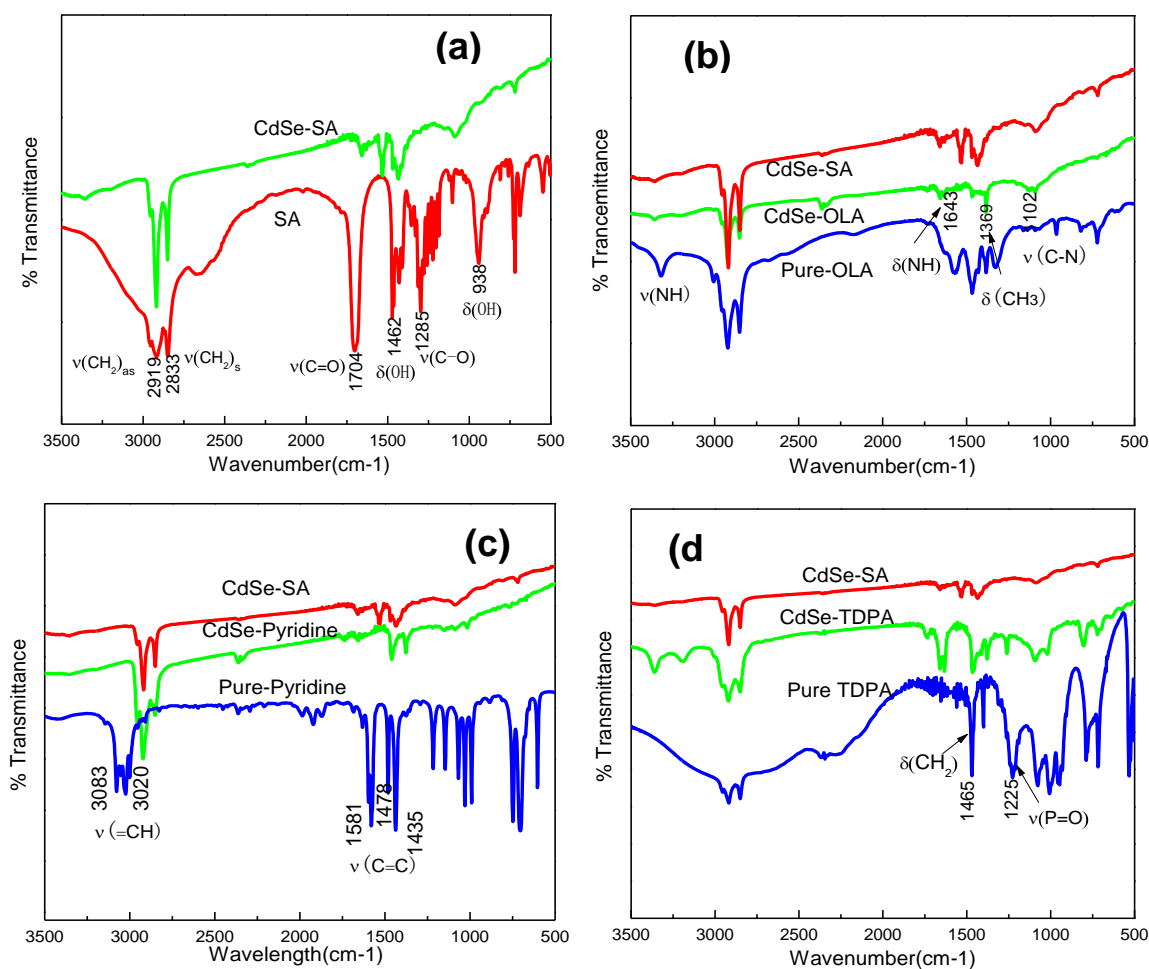
By Jinjin Liu<sup>1</sup>, Wanting Yang, Yunchao Li<sup>1,\*</sup>, Louzhen Fan<sup>1</sup>, and Yongfang Li<sup>2,\*</sup>

1. Department of Chemistry, Beijing Normal University, Beijing, 100875 (P. R. China)

2. Beijing National Laboratory for Molecular Sciences, CAS Key Laboratory of Organic Solids,  
Institute of Chemistry, Chinese Academy of Sciences, Beijing 100190 (P. R. China)

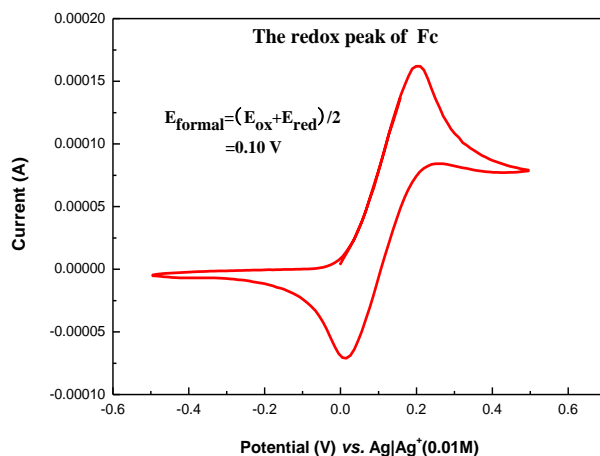


**Figure S1.** (a) CV curves of CdSe nanoparticles recorded under the same conditions but with different scan rate (a), (b) CV curves of CdSe nanoparticles recorded under the same conditions but with different scan directions (the arrows indicate initial scan direction), (c) CV curves of CdSe SNCs exposed to air for different time, (d) the optical pictures of a glass carbon electrode dip-coated with different amount of CdSe SNCs, (e) full-range XPS spectrum of the CdSe SNCs shown in (b), (f-g) XPS spectrum of Cd<sub>3d</sub> and Se<sub>3d</sub> core level from the CdSe SNCs shown in (c). The presence of quite weak Se oxide peak at 58.9 eV<sup>-1</sup> in (g), signifying the CdSe SNCs may partially oxidize when exposed to air.

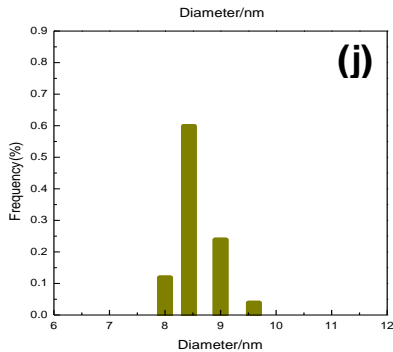
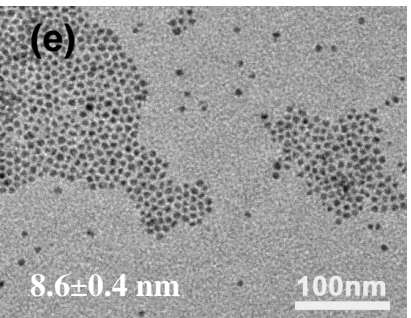
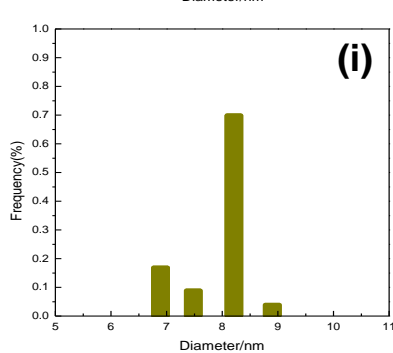
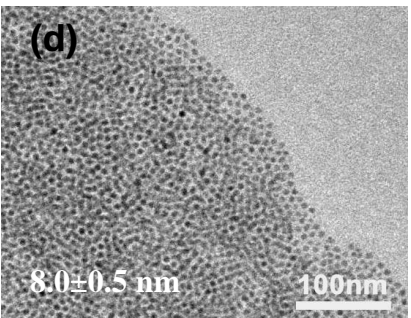
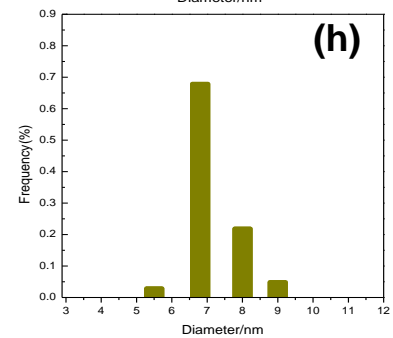
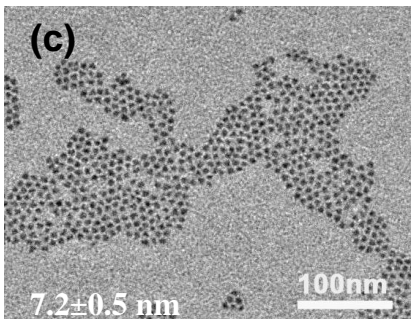
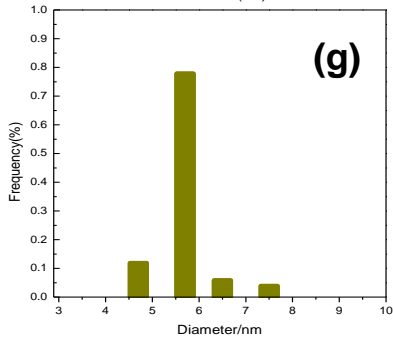
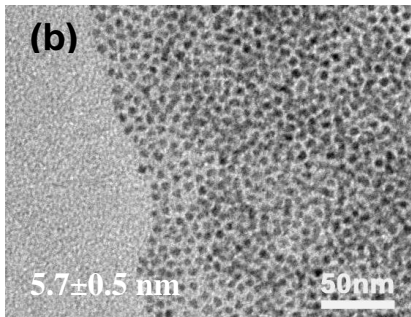
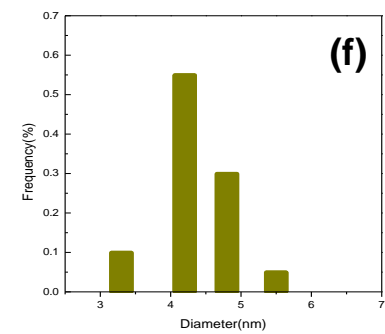
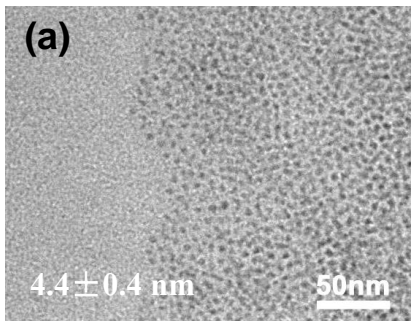


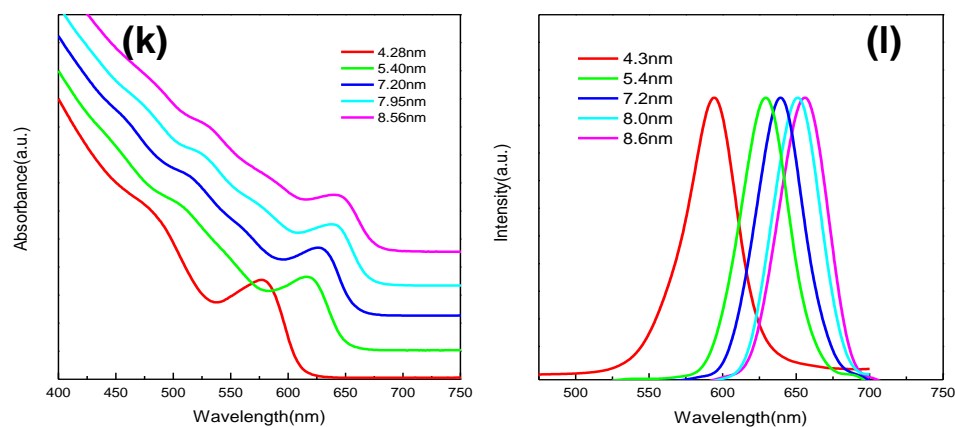
**Figure S2.** (a) FTIR spectra of free stearic acid (SA), and SA-capped CdSe SNCs ( the strong and characteristic peaks at 1435, 1662 and 3360 cm<sup>-1</sup> in the spectrum of the SA-capped CdSe

SNCs are assigned to the asymmetric and symmetric stretching vibration of a carboxylate group, and OH stretching vibration, respectively<sup>2-4</sup>, indicating that SA is the major ligand for the crude CdSe SNCs), (b) FTIR spectra of free oleylamine (OLA), and the CdSe SNCs with and without undergoing OLA exchange (the strong and characteristic peaks at 3359, 3148  $\text{cm}^{-1}$  are assigned to the stretching vibration of N-H bonds<sup>4-5</sup>, indicating OLA is the major ligand for the CdSe SNCs undergone such ligand exchange), (c) FTIR spectra of free pyridine, and the CdSe SNCs with and without undergoing pyridine exchange (the strong and characteristic peaks at 1457 and 1371  $\text{cm}^{-1}$  are assigned to the pyridine<sup>5</sup>, indicating pyridine is the major ligand for the CdSe SNCs undergone such ligand exchange); (f) FTIR spectra of free tetradecylphosphonic acid (TDPA), CdSe SNCs with and without undergoing TDPA exchange (the strong and characteristic peaks at 1250 and 3366  $\text{cm}^{-1}$  are assigned to the P=O and OH stretching vibration<sup>6-7</sup>, indicating TDPA is the major ligand for the CdSe SNCs undergone such ligand exchange).

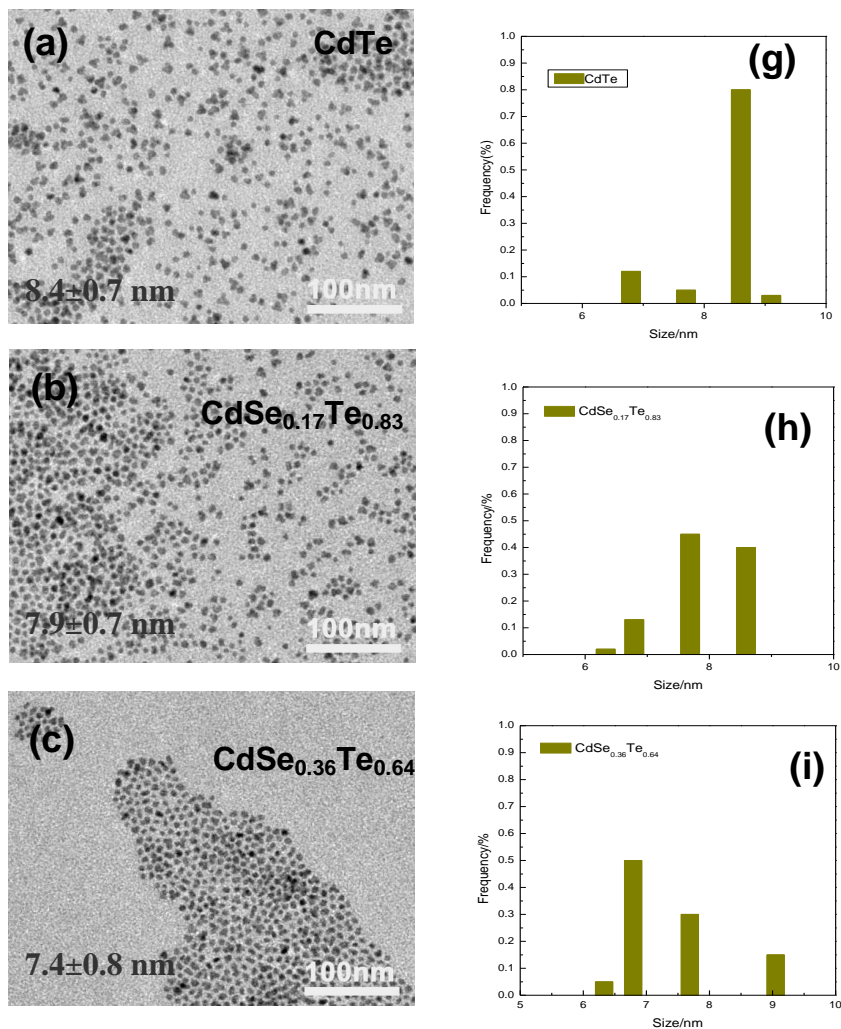


**Figure S3.** Cyclic voltammogram of ferrocene for determining the relative potential of the home-made Ag/Ag<sup>+</sup> (0.01 M AgNO<sub>3</sub> in acetonitrile) electrode.





**Figure S4.** (a-e) TEM images of CdSe SNCs with different sizes, (f-j) size distribution histograms corresponding to the CdSe SNCs shown in (a-e), (k-l) absorption and photoluminescence spectra of the CdSe SNCs with different sizes.





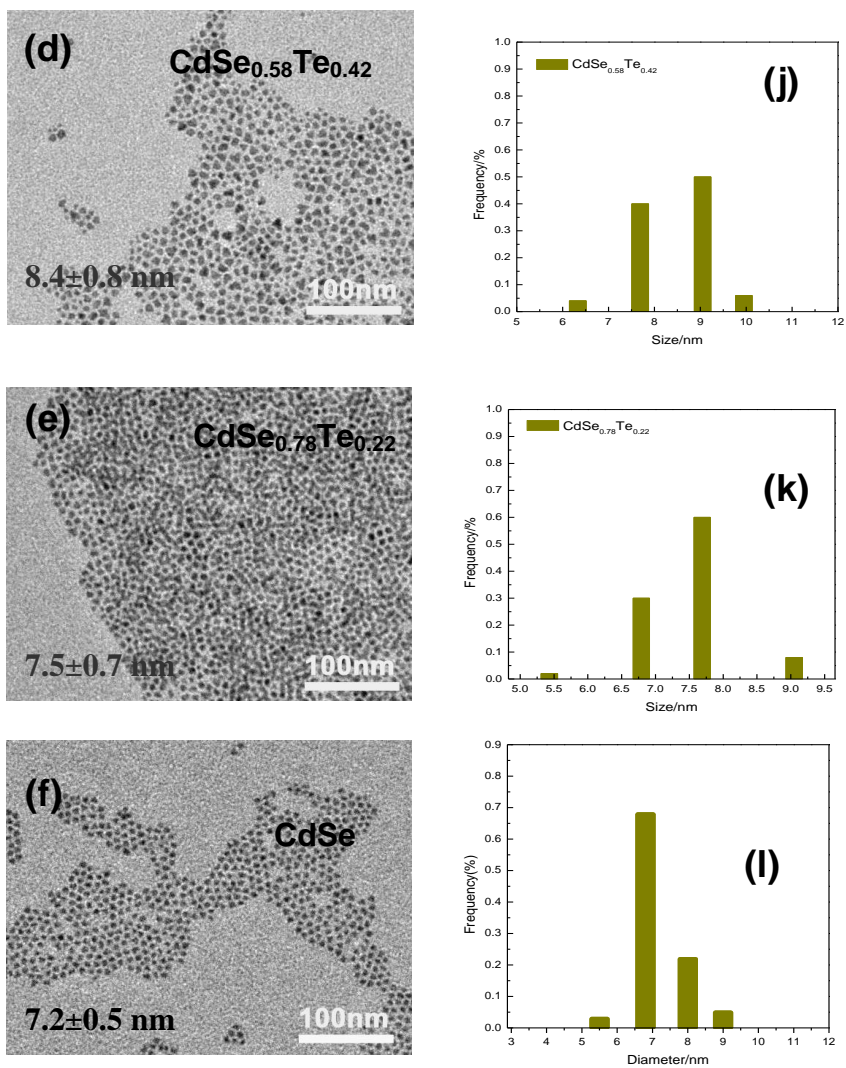


**Figure S5.** (a-f) TEM images of CdTe, alloyed CdSe<sub>x</sub>Te<sub>1-x</sub> (x=0.17, 0.36, 0.58, 0.78) and CdSe SNCs, (g-l) size distribution histograms corresponding to the SNCs shown in (a-f).

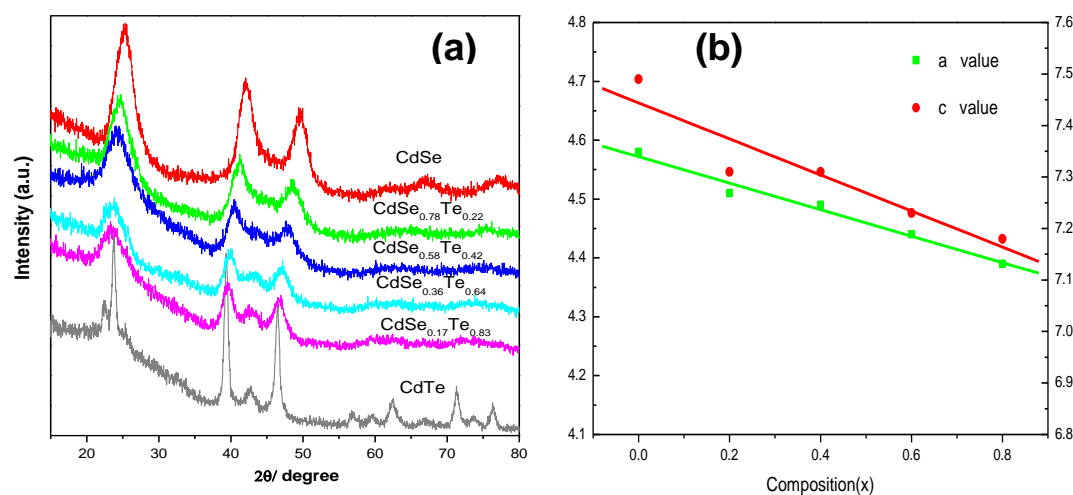


**Figure S6.** (a) Powder XRD patterns of CdSe<sub>x</sub>Te<sub>1-x</sub> (x=0, 0.17, 0.36, 0.58, 0.78 and 1.0) alloyed NCs, (b) The a-(■) and c-(●) axis values of the alloyed NCs as a function of Se content (x ).

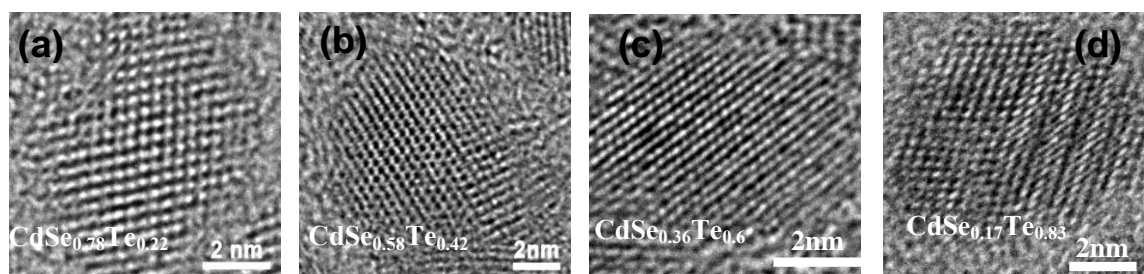


**Figure S7.** HRTEM images of alloyed CdSe<sub>x</sub>Te<sub>1-x</sub> SNCs with different Se composition, a) x= 0.78, b) x=0.58, c) x=0.36, d) x=0.17.

## References

- (1) Katari, J. E. B.; Colvin, V. L.; Alivisatos, A. P. X-ray Photoelectron Spectroscopy of CdSe Nanocrystals with Applications to Studies of the Nanocrystal Surface. *J. Phys. Chem.* **1994**, *98*, 4109-4117
- (2) Zhang, B.; Kong, T.; Xu, W.; Su, R.; Gao, Y.; Cheng, G. Surface Functionalization of Zinc Oxide by Carboxyalkylphosphonic Acid Self-Assembled Monolayers *Langmuir* **2010**, *26*, 4514-4522.
- (3) Wu, N. Q.; Fu, L.; Su, M.; Aslam, M.; Wong, K. C.; David, V. P. Interaction of Fatty Acid Monolayers with Cobalt Nanoparticles. *Nano Lett.* **2004**, *4*, 383-386.

- (4) Klokkenburg, M.; Hilhorst, J.; Erne, B. H. Surface analysis of magnetite nanoparticles in cyclohexane solution of oleic acid and oleylamine. *Vibrational Spectroscopy* **2007**, *43*, 243-248.
- (5) Jasieniak, J.; Califano, M.; Watkins, S. E. Size-Dependent Valence and Conduction Band - Edge Energies of Semiconductor Nanocrystals *ACS Nano* **2011**, *5*, 5888-5902
- (6) Luschtinetz, R.; Seifert, G.; Jaehne, E.; Adler, H.-J. P. Infrared Spectra of Alkylphosphonic Acid Bound to Aluminium Surfaces. *Macromol.Symp.* **2007**, *254*, 248-253.
- (7) Gao, W.; Dickinson, L.; Grozinger, C.; Morin, F. G.; Reven, L. Self-Assembled Monolayers of Alkylphosphonic Acids on Metal Oxides. *Langmuir* **1996**, *12*, 6429-6435.